J Appl Electrochem (2007) 37:1069–1075
DOI 10.1007/s10800-007-9357-6

ORIGINAL PAPER

Characterization of reactive magnetron sputtered nanocrystalline titanium nitride (TiN) thin films with brush plated Ni interlayer

B. Subramanian · M. Jayachandran

Received: 28 February 2007 / Revised: 15 June 2007 / Accepted: 21 June 2007 / Published online: 14 July 2007
© Springer Science+Business Media B.V. 2007

Abstract Thin nanocrystalline Titanium nitride (TiN) films were deposited on mild steel (MS) substrates using reactive direct current magnetron sputtering. With the aim of improving the corrosion resistance an additional Nickel interlayer of about 5 μm thick was brush plated on to the steel substrates. X-ray diffraction analysis showed the polycrystalline nature of the sputtered TiN films. SEM analysis showed uniform surface morphology with dense columnar structure. Laser Raman spectroscopy revealed the presence of characteristic peaks of TiN at 320, 440 and 570 cm^{-1}. The optical quality of the film was confirmed from the photoluminescence (PL) spectrum recorded at room temperature. The corrosion behavior of the coatings in 3.5% NaCl solution was studied using electrochemical techniques.

Keywords Corrosion resistance · Magnetron sputtering · PVD · Thin Films · Titanium Nitride

1 Introduction

Titanium Nitride (TiN) coatings prepared by physical vapor deposition (PVD) are increasingly used in various applications such as the tool industry, microelectronics, artificial jewelry, diffusion barriers and electrodes for chemical and thermal stability, because of their excellent properties such as extreme hardness, low electrical resistivity, high wear and excellent corrosion resistance and high thermal stability [1–5].

B. Subramanian (✉) · M. Jayachandran
ECMS Division, Central Electrochemical Research Institute, Karaikudi 630006, India
e-mail: tspsenthil@yahoo.com

TiN coatings have a tendency to failure, especially on softer substrates due to the fact that the substrate cannot provide effective support for the TiN coating. The poor adhesion to the substrate arises due to the difference in the surface morphological properties between the hard coating and the substrate [6]. Mild steel is used as a structural material in many applications. The existence of an interlayer is believed to alter the surface morphology and orientation of the substrate which enhances the adhesion strength to a larger extent.

Generally, techniques like physical vapour deposition (PVD)[7–9], plasma assisted chemical vapour deposition (PACVD), plasma enhanced chemical vapour deposition (PECVD) and hollow cathodic ionic plating [10] are used in developing hard coatings on various substrates. The disadvantage of physical vapor deposited TiN coatings is that they inherently possess columnar microstructures leading to a large number of pores in the coatings [11]. The columnar structure allows the pores to run across the coating thickness so that the corrosive medium may attack the coating/substrate intersurface [12]. It is, therefore, important to reduce the porosity of the coatings over which the hard coatings are deposited to improve the corrosion protection of the substrate.

Previous work showed that the surface of the sputtered TiN coating became smooth and the number and size of the particles also decreased through the use of pulsed bias [13]. Microstructure and nano indentation hardness of Ti/TiN-multilayer coatings deposited by reactive magnetron sputtering have been discussed [14]. An electroless nickel interlayer was employed in TiN films deposited onto low carbon steel and an increase in both surface hardness and adhesion strength in the as-derived $TiN/Ni_3P/Fe$ coating stack was observed [15]. The formation of an interface diffusion layer and a duplex composite layer at the inter-

face enhance the adhesion strength and hardness of the TiN composite coating [16].

In this investigation, structural, microstructural and optical properties of TiN layers and the corrosion resistance behavior of TiN/Ni/MS system were studied.

2 Experimental

2.1 Surface preparation of substrates and Ni Brush plating

The substrate used was MS, consisting of 0.37 wt% C, 0.28 wt% Si, 0.66 wt% Mn and 98.69 wt% Fe. Coupons of the substrate were cut to a size of 75 × 25 mm and the surface was ground with SiC paper to remove the oxides and other contamination. The polished substrates were degreased with acetone and then cathodically electro-cleaned in alkali solution containing sodium hydroxide and sodium carbonate for 2 min at 70 °C, followed by rinsing with distilled water. After cathodic cleaning the substrates were subsequently dipped in 5 vol.% H_2SO_4 solution for 1 min and thoroughly rinsed in distilled water.

A microprocessor controlled Selectron Power Pack Model 150A—40 V was used to transform AC current to DC. The schematic of the brush plating system is given in Fig. 1. The electrolyte, similar to a Watt's bath, contained 240 g l^{-1} nickel sulphate, 40 g l^{-1} nickel chloride and 30 g l^{-1} boric acid. The pH and temperature was maintained at 4.0 and 28 °C (RT), respectively. Figure 2 shows a cyclic voltammogram obtained for Ni solution. Ni deposition takes place at –1.0 V and two stripping peaks are noted at +0.25 and +0.75, which indicates that the bath behaves similarly to the usual Watts bath.

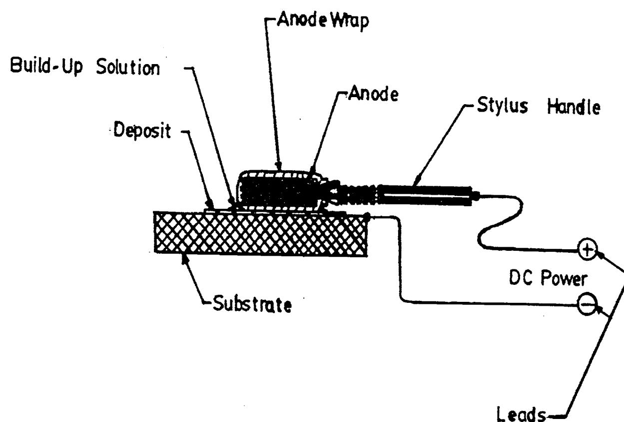

Fig. 1 Schematic of the brush plating process

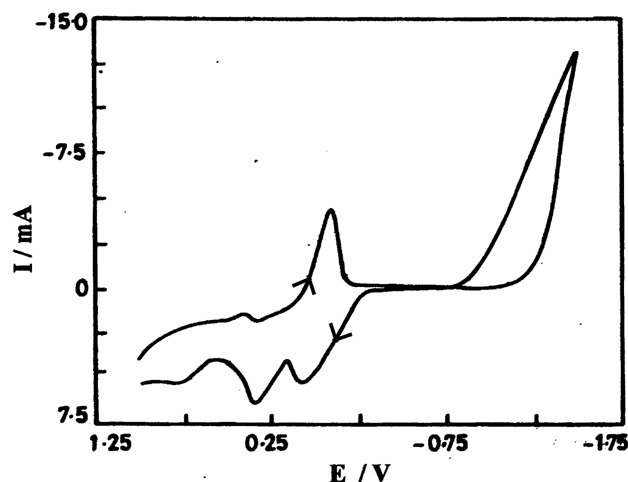

Fig. 2 Cyclic voltammogram of Ni salt containing solution

2.2 Sputter deposition of titanium nitride thin films and characterization

The layers of TiN were deposited on well-cleaned MS substrates using a dc magnetron sputter deposition unit (HINDHI VAC). The base vacuum of the chamber was below 10^{-6} Torr (1.33×10^{-4} Pa) and the substrate temperature was kept at 400 °C. High purity argon was fed into the vacuum chamber for the plasma generation. The substrates were etched for 5 min at a dc power of 50 W and an argon pressure of 10 mTorr (1.33 Pa). A high purity (>99.999%) Ti target of 7.5 cm in diameter was used as cathode. The deposition parameters for TiN sputtering are summarized in Table 1.

The deposited films were analyzed for crystallographic structure with a X Pert Pro diffractrometer using CuKα line. The microstructure of the coatings was examined using a Hitachi S 3000 H scanning electron microscope and a Nanoscope Atomic Force Microscope. Micro hardness of the films on MS was evaluated using a DM-400 micro hardness tester from LECO with Vickers indenters. A dwelling time of 15 s and a load of 25 gf and 5 gf were used for the

Table 1 Deposition parameters for TiN reactive sputtering

Objects	Specification
Target	Ti (99.999%)
Substrate	Mild Steel (MS)
Target to substrate distance	60 mm
Ultimate vacuum	1×10^{-6} m bar
Operating vacuum	2×10^{-3} m bar
Sputtering gas (Ar:N_2)	50:50
Power	250 W
Substrate temperature	400 °C

measurement. The excitation wavelength was 632.8 nm for Raman measurements. The data were collected with a 10 s data point acquisition time in the spectral region 200–1200 cm^{-1}. The Photoluminescence measurements were made using a Cary Eclipse Fluorescence Spectrophotometer (VARIAN) employing PbS photo-detector and a 150 w Xe arc discharge lamp as the excitation light source.

2.3 Electrochemical corrosion testing

Electrochemical polarization studies were carried out using a BAS IMG Electrochemical analyzer. Experiments were conducted using a standard three-electrode configuration with a platinum foil as the counter electrode, a saturated calomel electrode (SCE) as the reference electrode and the sample as the working electrode. The specimen (1.0 cm^2 exposed area) was immersed in the test solution of 3.5% NaCl. Experiments were carried out at room temperature (28 °C). In order to establish the open circuit potential (OCP), prior to measurements, the sample was immersed in the solution for about 60 min.

Impedance measurements were conducted using a frequency response analyzer. The spectrum was recorded in the frequency range 10 mHz–100 kHz. The applied alternating potential had root mean square amplitude of 10 mV on the open circuit potential. After reaching the stable OCP, the upper and lower potential limits of linear sweep voltametry were set at ±200 mV with respect to OCP and the sweep rate was 1 mV s^{-1}. The Tafel plots were obtained after the electrochemical measurements. The porosity was determined from the polarization resistance and corrosion potential deduced from the potentiodynamic polarization technique using the relation [17]

$$P = \left(R_{ps}/R_p\right) \times 10^{-|\Delta E_{corr}|/b_a} \tag{1}$$

where P is the total coating porosity, R_{ps} is the polarization resistance of the MS substrate, R_p is the polarization resistance of the coating, ΔE_{corr} is the difference between the corrosion potentials of the coating and the bare MS substrate and b_a is the anodic Tafel slope of the substrate.

3 Results and discussion

3.1 Structure and micro hardness

The X-ray diffraction patterns obtained for the reactive sputter deposited titanium nitride films on MS substrates with and without Ni interlayer using the Ar/N_2 ratio of 50:50 (Fig. 3) indicate the successful formation of TiN which has a cubic crystal structure with a lattice parameter of a = 4.23 nm. The observed inter planar distances 'd'

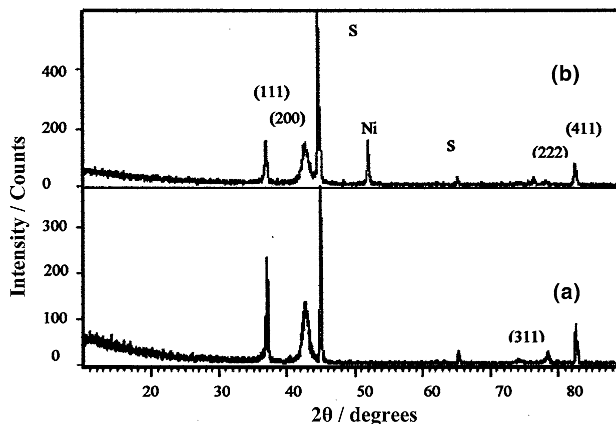

Fig. 3 X-ray diffractogram of sputtered TiN film on (a) MS (b) Ni on MS

(hkl) are in very good agreement with the standard 'd' values (ICDD No 03-065-5774). The peaks at 36.78 and 42.53 correspond to diffraction along (111) and (200) planes and these peaks agree well with the standard XRD data of TiN. When the ratio of Ar/N_2 was varied as 20:80 and 80:20, the pattern showed only a slight change in the intensity of (100) orientation.

The grain size of the coatings was determined by the equation

$$D = \frac{0.94\lambda}{\beta \, \mathrm{Cos}\theta} \tag{2}$$

where D is the grain size, β is the full width at half maximum (FWHM) of the diffraction peak, λ is the wavelength of the incidental CuKα X ray (1.514 Å), and θ is the diffraction angle. The grain size of the film was found to be about 80 nm. Such a small grain size contributes to the smooth surface morphology and also may have a beneficial effect on improvement of the micro- hardness of the coating [14]. Also the grain size reduction to the nanometer range results in considerable improvement in localized corrosion resistance [15].

The micro-strain (ε) was calculated from the relation [16]

$$\varepsilon = \beta \, \mathrm{Cos}\theta/4 \tag{3}$$

The dislocation density (δ) [16], defined as the length of the dislocation per unit volume of the crystal, was calculated from

$$\delta = 15 \, \varepsilon/a \, D \tag{4}$$

The value of micro strain (ε) and the dislocation density (δ) of the as grown film were found to be 6.7×10^{-4} and 3.5×10^{14} cm^{-2}.

The surface micro hardness values of TiN film on MS, having a thickness of 1.2 μm, increased from about 1020 HV to 1750 HV when the applied load was decreased from 25 gf to 5 gf.

3.2 Micro structure analyses

The microstructure of the TiN film on the Ni interlayer prepared with an Ar/N_2 ratio of 50:50 is shown in Fig. 4a. The structure consists of grains of about 200 nm size which have aggregates of many crystallites. The characteristic feature of TiN coating is the presence of micro defects like pin holes. The cross-sectional SEM photograph of TiN film deposited under optimized conditions is shown in Fig. 4b. It is evident that the TiN films have a columnar structure with voids and boundaries throughout the film thickness. This growth process is similar to that reported in the literature for TiN films [17].

The surface topography of the TiN thin films was studied using Atomic Force Microscopy (AFM). The result for a scanned area of 2 × 2 μm and is shown in Fig. 5. The AFM image reveals that its growing surface is compact and characterized with a cellular-like pattern. From the horizontal cross section analysis the minimum and maximum grain size was estimated to be about 80 nm.

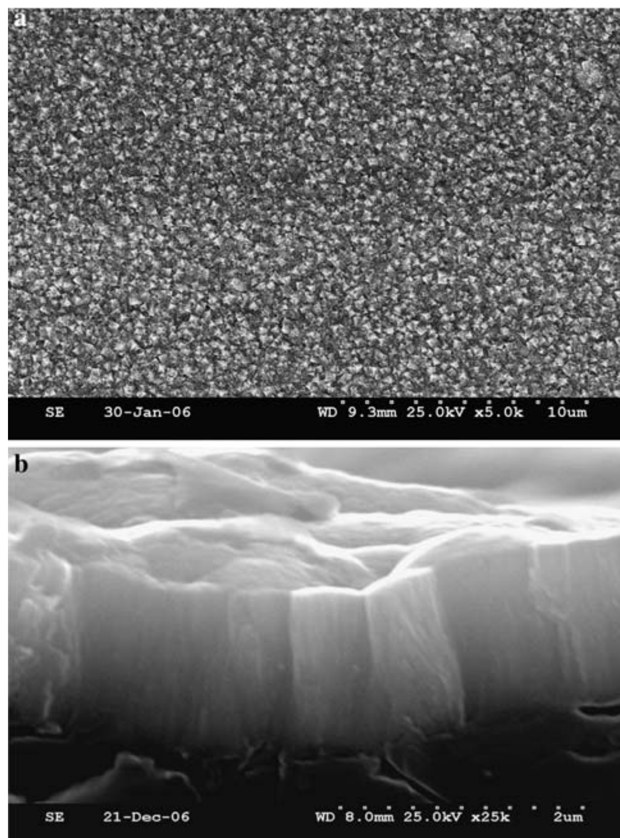

Fig. 4 SEM of sputtered titanium nitride thin film (**a**) Plane view (**b**) Cross sectional view

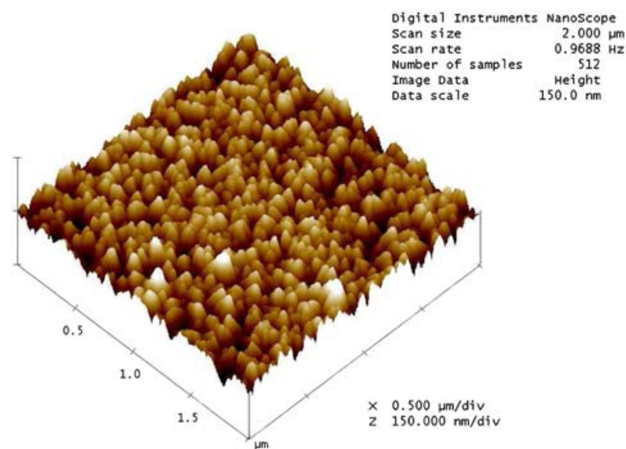

Fig. 5 Representative AFM image showing the topography of TiN film

The value of the mean roughness R_a was calculated as the deviations in height from the profile mean value [18]. The roughness value estimated from these images is 5.2 nm, which shows that the films are very smooth and have uniform grain size distribution all over the surface.

3.3 Reflectance and Laser Raman studies

The reflectance of the TiN coatings was measured with a double beam spectrophotometer. A sputtered aluminium surface was used as the standard mirror. The reflectance measured was the so-called relative reflectance. A typical reflectance spectrum was taken in the wavelength region of 200–2000 nm of a titanium nitride film on MS substrate as shown in Fig. 6. These films show a maximum reflectance of about 60% at 850 nm which is in good agreement with the value of 65% reported for TiN films produced by unfiltered arc sources and 80% for films prepared by filtered arc evaporation [19].

Raman spectra of TiN film shows the characteristic peaks at 320, 440, and 570 cm^{-1}, which are assigned to transverse acoustic (TA)/longitudinal acoustic (LA), second-order acoustic (2A), and transverse optical (TO) modes of TiN, respectively. This is in good agreement with the reported Raman studies for TiN films reported by Constable et al. [20]. The phonon bands in the acoustic and optic range are due to the vibrations of the heavy Ti ions (typically 150–300 cm^{-1}) and the lighter N ions (typically 400–650 cm^{-1}) respectively (Fig. 7).

A PL spectrum recorded at room temperature for the TiN/MS system is shown in Fig. 8. It is interesting to note that emissions appearing at 482 and 531 nm are only in the visible region for excitation at 390 nm. This implies that

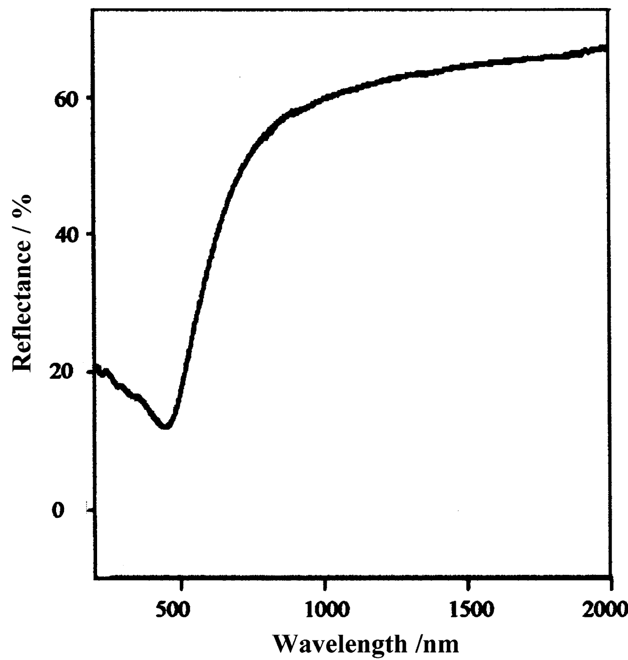

Fig. 6 Reflectance of titanium nitride film deposited on MS

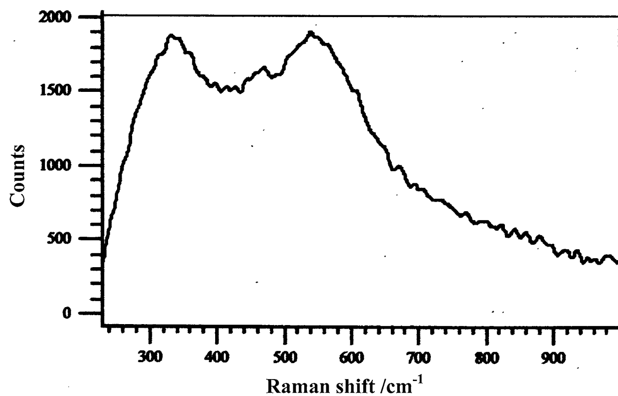

Fig. 7 Laser Raman Spectrum for titanium nitride film

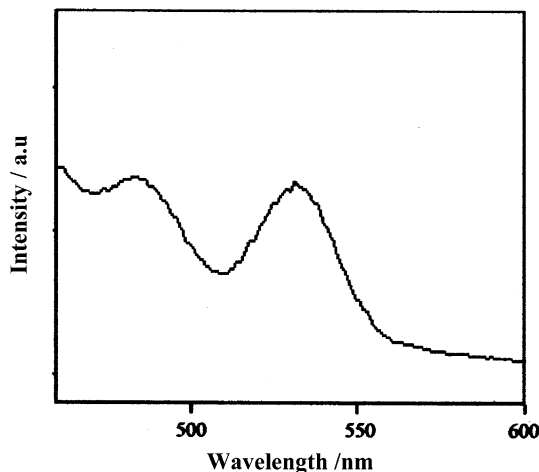

Fig. 8 Photoluminescence spectrum magnetron sputtered titanium nitride film

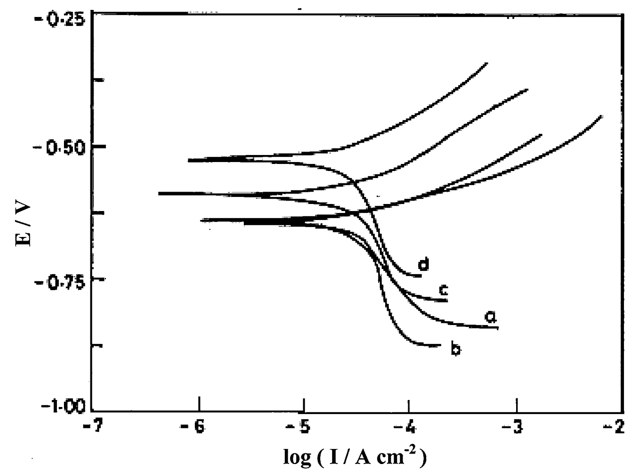

Fig. 9 Polarization studies of (a) blank MS (b) TiN on MS (c) Ni on MS (d) TiN/Brush plated Ni/MS in 3.5% w/v NaCl

the titanium nitride films prepared by dc reactive magnetron sputtering are of good optical quality.

3.4 Potentiodynamic polarization and AC impedance spectroscopy

The principal aim of this investigation was to study surface degradation resulting from electrochemical processes and this necessitated an analysis of the surface deposit left after electrochemical reactions. The potentiostatic polarization experiments provided some idea about the electrochemical activity of the material. However, it necessitated scanning across a wide range of electrode potentials so that the surface of the material at the end of such polarization was the result of cumulative effects at different potentials. To analyze the surface the material was subjected to potentiostatic polarization one specified potential being impressed on the material at a time. The potentials were either anodic or cathodic with respect to the primary electrochemical process occurring on the surface as indicated by the potentiostatic polarization curves. The corrosion rate (CR) is expressed in mils per year (mpy) [21].

$$CR = 0.1288 \times i_{corr} \times w/\rho \quad (5)$$

where i_{corr} is the corrosion current in A cm^{-2}, w is the equivalent weight of metal and ρ is the metal density.

Typical polarization curves obtained for the corrosion behavior of the TiN sputtered MS samples are shown in Fig. 9. Table 2 gives the results of corrosion testing for the MS substrate, TiN/MS and TiN/brush plated Ni/MS stack. For the TiN/brush plated Ni/MS stack the corrosion current is observed to be the lowest, 0.84×10^{-5} A cm^{-2}, as indicated in Table 2. The corrosion current is as high as 3.31×10^{-5} A cm^{-2} for the TiN/MS system in which the

Table 2 Corrosion parameters obtained from polarization studies in 3.5% w/v NaCl

Sample	E_{Corr} vs. SCE/mV	ba/V dec^{-1}	bc/V dec^{-1}	I_{Corr}/A cm^{-2} 10^{-5}	Corrosion rate/mpy 10^{-5}
MS substrate	–0.651	0.064	–0.164	5.61	2.56
TiN on MS	–0.649	0.085	–0.550	3.31	2.05
Ni on MS	–0.568	0.092	–0.493	2.96	1.25
TiN/brush plated Ni/MS	–0.504	0.101	–0.578	0.84	1.01

rapid corrosion of iron takes place at the cavities of the TiN coating owing to the combined effect of the rather noble steady-state potential of the TiN coating and the relatively active iron species. Consequently, the corrosion of MS is accelerated in spite of the TiN coating. However, in the TiN/brush plated Ni/MS stack the brush plated Ni interlayer tends to act as a barrier which effectively retards the corrosion of iron.

The same three-electrode cell stack, as used for the potentiodynamic polarization experiments, was employed for the AC impedance investigations. Impedance measurements were made at open circuit potential (OCP) applying an AC signal 10 mV in the frequency range 10 Hz to 1 MHz. The Nyquist and Bode plots for the samples used for corrosion tests in 3.5% w/v NaCl solution are shown in Figs. 10 and 11, respectively. The double layer capacitance C_{dl} value is obtained from the frequency at which Z imaginary is maximum [21]

$$\omega(Z_{(im)}\max) = 1/C_{dl}R_{ct} \tag{6}$$

The increase in R_{ct} values and decrease in C_{dl} values as shown in Table 3 for the TiN/brush plated Ni/MS stack confirm the better corrosion resistance of these systems compared to TiN/MS and bare MS substrate. A more semicircular region in the case of the TiN/brush plated Ni/MS stack indicates that this system has maximum corrosion resistance, as observed from the high frequency region of the impedance spectra. The porosity of the nitride metal coatings with brush plated Ni interlayer is found to be lower than that of the coatings without Ni interlayer.

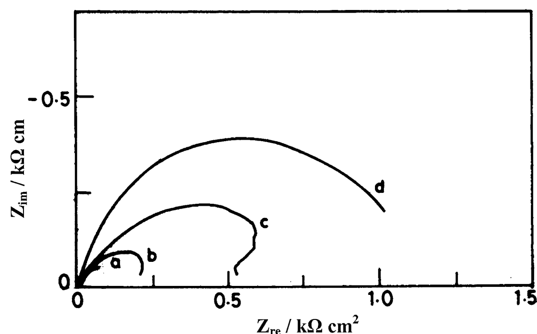

Fig. 10 Nyquist plots for corrosion measurements of (a) blank MS (b) TiN on MS (c) Ni on MS (d) TiN/Brush plated Ni/MS in 3.5% w/v NaCl

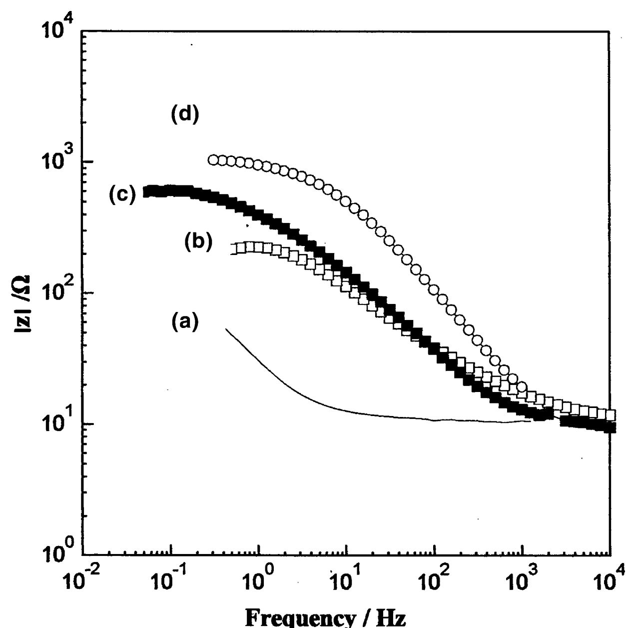

Fig. 11 Bode plots (a) blank MS (b) TiN on MS (c) Ni on MS d) TiN/Brush plated Ni/MS

4 Conclusions

Titanium nitride (TiN) films were successfully grown on Ni/MS and MS substrates by reactive DC magnetron sputtering. Structural analysis using XRD reveals that the films are polycrystalline in nature possessing cubic structure and having the lattice parameter value a = 4.23 nm. A dense columnar structure is observed from SEM and AFM analyses. The films show a maximum reflectance of about 60% at 850 nm. The characteristic Raman peaks confirm the formation of TiN films. Peaks at 320, 440, and 570 cm^{-1}were observed in the Raman spectra of the films. From electrochemical results, supported by microstructural observations, it can be concluded that the TiN/brush plated Ni/MS stack has better corrosion resistance properties compared with TiN/MS and bare MS systems.

Table 3 Corrosion parameters obtained from impedance measurements by Nyquist plots

Sample	OCP/V	R_{ct} Ohm cm^2	C_{dl}/F cm^{-2}	Porosity/(%)
MS substrate	–0.569	62.2	7.732×10^{-3}	–
TiN on MS	–0.550	193.4	2.005×10^{-4}	2.08×10^{-1}
Ni on MS	–0.543	675.2	2.581×10^{-4}	4.64×10^{-3}
TiN/brush plated Ni/MS	–0.493	1171.3	2.555×10^{-5}	2.68×10^{-4}

Acknowledgements One of the authors (B.S) thanks the Department of Science &Technology, New Delhi, for a research grant under SERC Fast Track scheme No SR/FTP/CS-23/2005.

References

1. Grips WVK, Ezhil Selvi V, Barshilia HC, Rajam KS (2006) Electrochim Acta 51:3461
2. Souto RM, Alanyali H (2000) Corr Sci 42:2201
3. Kim TS, Park SS, Lee BT (2005) Mater Lett 59:3929
4. Dobrzanske LA, Adamiak M (2003) J Mater Process Technol 133:50
5. Hogmark S, Jacobson S, Larsson M (2000) Wear 246:20
6. Hu SB, Tu JP, Mei Z, Li ZZ, Zhang XB (2001) Surf Coat Tech 141:174
7. Hainsworth SV, Soh WC (2003) Surf Coat Tech 163:515
8. Na HD, Parka HS, Junga DH, Leea GR, Joob JH, Leena JJ (2003) Surf Coat Tech 169–170:41
9. Combadiere L, Machel J (1996) Surf Coat Tech 88:17
10. Li Y, Li Q, Wang F (2003) Corr Sci 45:1367
11. Barshilia HC, Prakash MS, Poojari M, Rajam KS (2004) Trans Inst Met Fin 82(3–4):123
12. Jehn HA (2000) Surf Coat Tech 125:212
13. Huang MD, Lin GO, Zhao YH (2003) Surf Coat Tech 176:1367
14. Li TS, Li H, Pan F (2001) Surf Coat Tech 137:225
15. Haichuan Mu, Jin Seok, Lin RY (2003) J Electrochem Soc 150(2):c67
16. Hu SB, Tu JP, Mei Z, Li ZZ, Zhang XB (2001) Surf Coat Tech 141:174
17. Hones P, Zakri C, Shmid PE, Lery F, Shojel OR (2000) Appl Phys Lett 76:3194
18. Jacobs MH (1986) Surf Coat Tech 29:221
19. Elsener B, Rota A, Bohni H (1989) Mater Sci Forum 44–45:28
20. Constable CP, Yarwood J, Münz WD (1999) Surf Coat Tech 116–119:155
21. Venketachari G (1982) Corr Bull 2:14